



# Spin–Orbit Resonances of High-eccentricity Asteroids: Regular, Switching, and Jumping

Valeri V. Makarov<sup>1</sup> , Alexey Goldin<sup>2</sup>, and Dimitri Veras<sup>3,4,5</sup> <sup>1</sup> U.S. Naval Observatory, 3450 Massachusetts Ave., Washington, DC 20392-5420, USA; [valeri.makarov@gmail.com](mailto:valeri.makarov@gmail.com)<sup>2</sup> Teza Technology, 150 N. Michigan Ave., Chicago IL 60601, USA; [alexey.goldin@gmail.com](mailto:alexey.goldin@gmail.com)<sup>3</sup> Centre for Exoplanets and Habitability, University of Warwick, Coventry CV4 7AL, UK<sup>4</sup> Department of Physics, University of Warwick, Coventry CV4 7AL, UK; [d.veras@warwick.ac.uk](mailto:d.veras@warwick.ac.uk)

Received 2020 September 1; revised 2021 March 3; accepted 2021 April 15; published 2021 June 10

## Abstract

Few solar system asteroids and comets are found in high-eccentricity orbits ( $e > 0.9$ ), but in the primordial planetesimal disks and in exoplanet systems around dying stars such objects are believed to be common. For 2006 HY51, the main belt asteroid with the highest known eccentricity 0.9684, we investigate the probable rotational states today using our computer-efficient chaotic process simulation method. Starting with random initial conditions, we find that this asteroid is inevitably captured into stable spin–orbit resonances typically within tens to a hundred megayears. The resonances are confirmed by direct integration of the equation of motion in the vicinity of endpoints. Most resonances are located at high spin values above 960 times the mean motion (such as 964:1 or 4169:4), corresponding to rotation periods of a few days. We discover three types of resonance in the high-eccentricity regime: (1) regular circulation with weakly librating aphelion velocities and integer-number spin–orbit commensurabilities, (2) switching resonances of higher order with orientation alternating between aligned (0 or  $\pi$ ) and sideways ( $\pi/2$ ) angles at aphelia and perihelia, (3) jumping resonances with aphelion spin alternating between two quantum states in the absence of spin–orbit commensurability. The islands of equilibrium are numerous at high spin rates but small in parameter space area, so that it takes millions of orbits of chaotic wandering to accidentally entrap in one of them. We discuss the implications of this discovery for the origins and destiny of high-eccentricity objects and the prospects of extending this analysis to the full 3D treatment.

*Unified Astronomy Thesaurus concepts:* [Eccentricity \(441\)](#); [Asteroids \(72\)](#); [Orbital resonances \(1181\)](#)

## 1. Introduction

Some asteroids in the solar system have eccentricities above 0.95. Their origin and destiny are not clear. They may be remnants of the primordial asteroid belt, results of relatively recent interaction with planets, or even captured interstellar objects. At such high eccentricities, triaxial celestial bodies can acquire very high prorated spin rates over billions of years of chaotic evolution (Makarov & Veras 2019), resulting in a rotational breakup and destruction. The most notable high-eccentricity object in the JPL Horizons database is 2006 HY51 with an eccentricity of 0.9684,<sup>6</sup> but a few other objects with slightly smaller eccentricity have been detected. These Apollo-class asteroids are near-Earth objects. Similar objects were involved in the bombardment of inner planets and accretion of primordial terrestrial planets. Around white dwarf planetary systems, highly eccentric asteroids are thought to be the primary progenitor of debris disks (Jura 2003; Debes et al. 2012; Veras et al. 2014, 2020; Malamud & Perets 2020a, 2020b) and observed metallic pollution in the photospheres of host stars (Zuckerman et al. 2010; Koester et al. 2014).

Minor planets are markedly nonspherical, and many of them, especially the larger ones, can be well approximated with triaxial ellipsoids. This idealized model is dynamically represented by three unequal, mutually orthogonal moments of inertia  $A$ ,  $B$ , and

$C$ , in increasing order. The values are not readily available from observations or remote measurements but can be estimated from the shape elongation parameters assuming uniform mass density or a certain density profile. There is a tendency for the dimensionless degree of triaxiality  $\sigma = (B - A)/C$  to increase with decreasing size and mass as we move from terrestrial planets to moons, minor planets, and comets. Potato-like shapes become prevalent in the domain of comets and asteroids, with  $\sigma$  becoming of the order of 0.1 and larger. The prolate shape and the gradient of gravitational potential from the central body give rise to a time-variable torque, which depends on the orientation of the asteroid with respect to the perturber. The corresponding equations of motion (Euler’s equations) comprise a set of three second-order nonlinear differential equations, which include the instantaneous direction cosines of the longest axis and the instantaneous spin rates about all three principal axes (Danby 1962). A 1D analog of this system is obtained for the planar case of zero obliquity when the principal axis of inertia (corresponding to the moment  $C$ ) is always orthogonal to the orbital plane (e.g., Goldreich & Peale 1966).

In this paper, we investigate the rotational states of high-eccentricity triaxial objects in the basic 1D model (i.e., regarding only the spin about the principal axis of inertia) on the example of 2006 HY51, the most eccentric asteroid on a closed orbit in the solar system. With a period of 4.17 yr and semimajor axis of 2.59 au, this asteroid spends most of the time at great distances from the Sun, experiencing vanishingly small external torque and, hence, rotating practically at a constant rate. The situation changes dramatically when it flashes through the perihelion at the closest separation 0.082 au, where a short but powerful burst of interaction changes its spin in a shock-like manner. The direction of this pulse depends mostly on the

<sup>5</sup> STFC Ernest Rutherford Fellow.<sup>6</sup> <https://ssd.jpl.nasa.gov/sbdb.cgi#top>

orientation angle at the point of closest approach, but the amplitude of impulse also depends on the current spin rate. The result is a strongly chaotic process, which was theoretically deduced even for much lower eccentricities (Wisdom et al. 1984; Wisdom 1987).

The chaotic 1D spin evolution was investigated in Makarov & Veras (2019) by direct integration with stiffness switching. In that paper, however, evolution was limited to a timescale that is roughly six orders of magnitude shorter than the current age of the solar system due to the slow and sequential integration, which cannot be parallelized. A computer-efficient and fast alternative technique is described in Makarov et al. (2020), which allows running parallel simulation trials spanning gigayears. This method takes advantage of the deterministic mapping between the two phase-space parameters on the scale of a single orbit, the orientation angle  $\theta$  at the time of aphelion, and the update of rotation velocity resulting from the perihelion impulse. We used the higher-fidelity version of the method, which is computationally more demanding, involving double interpolation mapping of the aphelion parameter space.

This paper is organized as follows. In Section 2, we briefly describe the computation for 2006 HY51 that led us to the discovery of multiple stable spin-orbit resonances. These resonances are confirmed by numerical integration with initial parameters in the vicinity of selected points of equilibrium in Section 3, and parameter space cross sections are mapped for some of them. Three different kinds of high-spin resonances are described in Section 4, one of which is not spin-orbit commensurate. Conclusions are drawn and possible directions of future research are discussed in Section 6.

## 2. Long-term Simulations of Rotation

We made use of the more computer-intensive version of the fast-tuple generation method described in Makarov et al. (2020).<sup>7</sup> The basic idea is to replace the costly ODE integration with generation of  $\{d_{\omega,i}, \theta_{i+1}\}$  tuples for perihelion and aphelion times from precomputed 2D interpolation functions, which turn out to be smooth and well behaved in the domain of interest. In this paper,  $\theta$  is the orientation angle of the ellipsoidal asteroid's longest axis in the orbital plane, i.e., the angle between the axis of the smallest moment of inertia  $\mathcal{A}$  and the fixed line of apsides. Its time derivative,  $\omega = \dot{\theta}$ , is the sidereal rotation velocity, and  $d_{\omega}$  is the change of  $\omega$  between two consecutive aphelia. As in the original paper, the motion is confined to the orbital plane, the gravitational torque is always orthogonal to the orbital plane, and only the force from the Sun is considered, neglecting small perturbations from the planets or the YORP effect. Possible effects of YORP and external perturbations are briefly discussed in Section 3. Our main computation included 512 separate and independent random-seeded trials for  $2.5 \times 10^8$  orbits each, i.e., each was longer than 1 Gyr, assuming a triaxiality parameter  $\sigma = (B - A)/C = 0.2$ . It confirmed that 2006 HY51 could not come close to the rate of several thousand  $n$  required for rotational breakup, by roughly an order of magnitude. The unexpected result was that all 512 simulations ended up in equilibrium states (resonances) within the simulation time span. A long-term or indefinitely long equilibrium state characterized by an aphelion

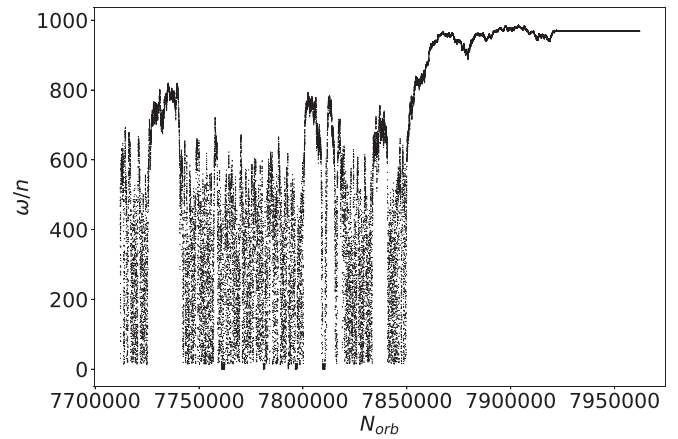


**Figure 1.** Simulated chaotic evolution of the rotation velocity of 2006 HY51 followed by a spontaneous capture into a commensurate spin-orbit resonance after  $7.92 \times 10^6$  orbits. A small segment of a simulation of  $2.5 \times 10^8$  orbits produced by the fast mapping method is shown.

spin rate varying within a finite range despite the powerful perturbations at perihelion passages, as opposed to rapidly changing chaotic rotation, is called a spin-orbit resonance in this paper. As we will see in the following, this equilibrium rotation state can be achieved even without an integer-number commensurability of the spin rate and orbital frequency. Numerically, once a state of this kind was achieved, our fast-tuple-generating simulation stopped behaving chaotically and remained within certain narrow ranges of phase-space parameters. Figure 1 shows the aphelion spin of a small segment of one such simulation. It depicts the peculiar character of spin evolution, when the random process appears to be bounded to a certain wide range of prograde velocities (approximately between  $12n$  and  $1100n$ ), transversing it relatively rapidly from one end to the other, and stalling for extended periods of time at the low end. These features are related to the remarkable distribution of impulses in the parameter space (see Figure 4 in Makarov & Veras 2019). Vanishingly small changes of velocity are possible when the process is cornered at the low bound adjacent to the separatrix. Likewise, although there is no fixed upper bound, the velocity updates become so small at high prograde velocities that the process may linger there for longer times. Returning to Figure 1, in one of such episodes, the asteroid suddenly stopped behaving chaotically and continued to rotate at a nearly constant aphelion rate.

Although the overall character and statistics of these long-term simulations are in excellent agreement with direct integration trials, the latter did not reveal the existence of resonances. The reason is that we performed only relatively short ( $10^5$  orbits) integrations, which are computationally heavy. Because of the rapid and powerful variation of the integrated parameters  $\theta$  and  $\omega$  within a small segment of the orbit around the perihelion, which takes only several days to cross, sufficiently accurate numerical results can be obtained with stiffness-switching methods, which automatically adjust the time step to the local gradient of the integrand. The process should be run for much longer time spans to see resonance captures. This means that the probability of random capture is low and it takes millions of orbits to accidentally hit one of the “stability islands.” Compared to the situation found by Wisdom et al. (1984) for solar system moons, we have a vast sea of

<sup>7</sup> A Julia script implementing this simulation is openly available at <https://github.com/agoldin/2006HY51>.

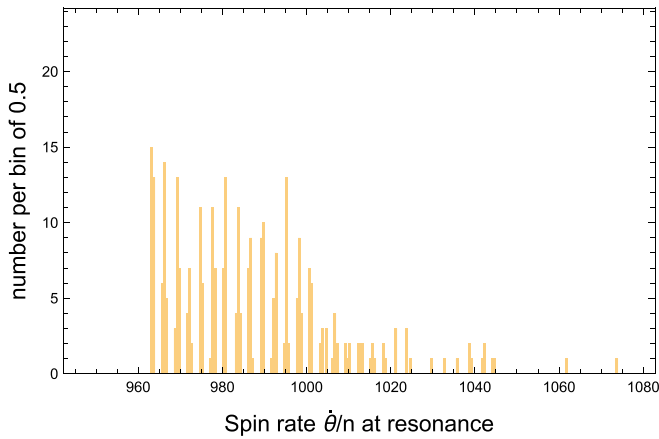


**Figure 2.** Histogram of end spin states of *regular* circulation resonances.

chaos with tiny islands of equilibrium interspersed in it at high eccentricity.

We can estimate the characteristic time of capture into resonance by counting the quantiles of the chaotic phase durations. Of the entire set of 512 simulations with random initial conditions, 25% were captured within  $2.5 \times 10^6$  orbits, and 50% within  $6.5 \times 10^6$  orbits. Thus, a significant fraction of trials show resonance capture within 20–50 million years. The resonance endpoints in  $\omega_{\text{ap}}/n$  are quantized with the lowest frequency around 963.5 (i.e., a 1927:2 resonance), except for a small fraction of trials that became stuck at the lower end of the  $\omega$  range. The resonance velocities of the majority high-spin endpoints are shown in Figure 2. We surmise that the characteristic time of capture into a specific resonance depends on the footprint in the parameter space.

### 3. Mapping Resonances of 2006 HY51

To verify the high-spin resonances discovered with the fast-tuple generation method, we performed exact numerical integration using some of the endpoints as initial conditions. One such deeper investigated resonance corresponds to a peak at the lower end of the distribution in Figure 2. The spin rate in this particular resonance displays a regular circulation behavior varying within a narrow range around  $\omega = 966.5n$ . The aphelion orientation angle modulo  $\pi$  circulates about 0, i.e., the asteroid is aligned with its longest axis with the direction to the Sun. The width of variation depends on the initial perturbation but is limited to the width of the resonance. The resonances that are seen as peaks in Figure 2 represent semi-integer spin-orbit commensurabilities, i.e.,  $\kappa:1$  and  $\kappa:2$ . A total of 90% of our trials that ended in one of the fixed- $\omega$  resonances did this in less than  $11 \times 10^6$  orbits, with a median duration of  $3.4 \times 10^6$  orbits.

Once we have identified the approximate location of high-spin resonances in the parameter space  $\{\theta_{\text{aphelion}}, \omega_{\text{aphelion}}\}$  using extensive simulations with the fast-tuple generation method, these tiny zones of equilibrium can be mapped in greater detail by direct numerical integration. Figure 3 shows a parameter space cross section (similar to a Poincaré map) at aphelion obtained from 20 integration trials of 200 orbits each with random initial parameters in the vicinity of the 964:1 resonance. It shows the actual half-width of the circulation island, which is 0.21 rad in  $\theta$  and 0.17n in  $\omega$ .

The islands of stable equilibrium are lined up in the  $\{\theta_{\text{aphelion}}, \omega_{\text{aphelion}}\}$  parameter space as beads on a string. Multiple resonances are found with  $\theta$  modulo  $\pi$  close to  $\pi/2$ , i.e.,

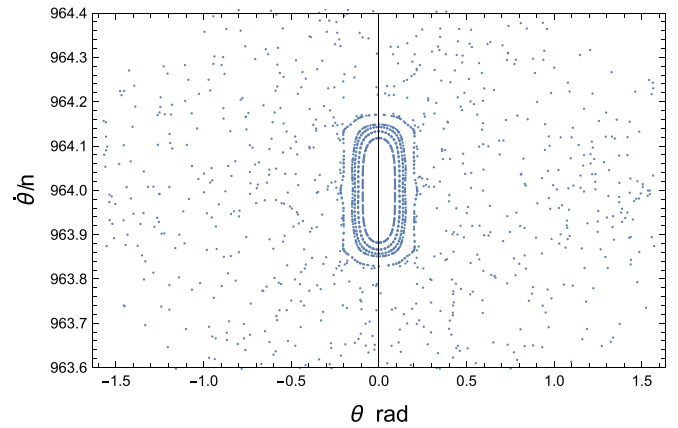


**Figure 3.** Aphelion parameter section of the 964:1 *regular* spin-orbit resonance of 2006 HY51 obtained by direct integration of motion.

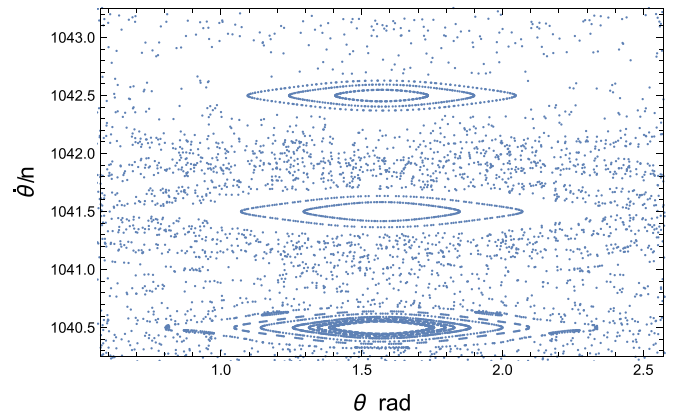


**Figure 4.** Aphelion parameter section of three adjacent spin-orbit resonances of 2006 HY51 with sidewise orientation of the asteroid and half-integer commensurabilities, obtained by direct integration of motion.

oriented sidewise at aphelia. This is not a new type of spin-orbit resonance since a sidewise capture into resonance has been discussed and deemed possible for the Moon, for example. These fixed- $\omega$  resonances, which we call *regular* in this paper, are characterized by a nearly zero net velocity update  $d_\omega$ , because the asteroid enters the periape with a  $\theta$  modulo  $\pi$  close to either 0 (aligned) or  $\pi/2$  (sidewise). A chain of half-integer resonances is mapped in Figure 4. Note that there are multiple resonances on both sides of this sequence outside of the plot.

The cross section and the very existence of a regular circulation resonance depend on the physical parameters  $\sigma = (B - A)/C$  and eccentricity  $e$ . We conducted a series of numerical experiments for the stable and well-defined 964:1 resonance (with the initial spin rate in close vicinity to  $\omega = 964n$ ). In the example shown in Figure 5, we start at the point of resonance with an initial aphelion angle  $\theta = \pi$ . To distinguish chaotic trajectories from stable resonance trajectories, we employ the chaos detection software implemented in Julia by Datsis (2018). The ODE of motion is integrated with two tangent perturbation vectors pointing from the original point to two random points  $\epsilon$  away for 100 orbits. The method uses the GALI(2) alignment index (Skokos et al. 2007), which in this 2D case computes the separation between the two perturbation vectors.<sup>8</sup> As chaotic behavior sets in, the initially

<sup>8</sup> Some explanations of how this method works can be found in [https://juliadynamics.github.io/DynamicalSystems.jl/latest/chaos/chaos\\_detection/](https://juliadynamics.github.io/DynamicalSystems.jl/latest/chaos/chaos_detection/).

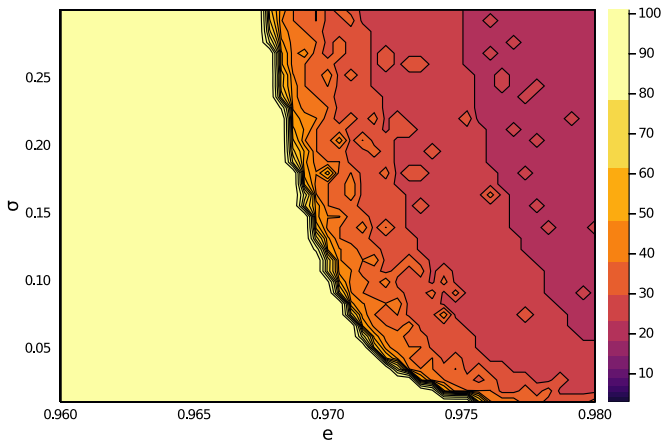


**Figure 5.** Areas of chaos (red colors) and stable spin-orbit resonance (yellow) of 2006 HY51 rotation in the  $\sigma$ - $e$  parameter space for initial aphelion conditions  $\theta(0) = \pi$ ,  $\omega(0) = 964 n$ . To distinguish chaotic and resonance trajectories, the number of orbits is computed (exponentially color-coded in this graph) for the GALI(2) index to fall below  $10^{-12}$ ; see text. Each integration was limited to 100 orbits.

orthogonal vectors become increasingly aligned approaching the direction of the strongest Lyapunov eigenvector. The decay of the area (or distance in this case) between the vectors is exponential for chaotic trajectories, but it follows a power law for deterministic trajectories. We empirically set the GALI(2) index threshold at  $10^{-12}$ . The contour plot shows the number of orbits required for the alignment of tangent vectors to drop below the threshold. The power-law decay for resonance trajectories is too slow to reach the threshold within the 100 orbits; hence, such trials end up in the saturated yellow-colored area of the graph. Figure 5 shows that the boundary between chaotic and resonance states in the  $\sigma$ - $e$  space is very sharp, and this commensurate spin-orbit resonance exists only if the triaxiality and eccentricity are sufficiently low. With  $\sigma = 0.2$  assumed for our fast-tuple generation numerical simulations, 2006 HY51 is located close to the boundary on the left-hand side, just enough for the stable 964:1 circulation resonance to emerge.

In the solar system, as well as in other stellar configurations, asteroids are subject to external variable forces, or perturbations, apart from the gravitational attraction from the star. The width of resonances depicted in Figures 3 and 4 defines the level of perturbation required to remove the object from an equilibrium state. For example, an external acceleration that changes the spin rate by more than  $0.17 n$  on the timescale of one orbit would probably be sufficient to drive 2006 HY51 out of the 964:1 spin-orbit resonance. The distribution of main belt asteroid rotation periods is fairly wide and limited on the high end by approximately 2.4 hr (Hestroffer et al. 2019) for radii greater than approximately 0.1 km, with most of the objects spinning quite fast. The high rates of rotation are commonly attributed to the secular YORP acceleration, which is caused by irregularities in the asteroid’s shape, solar irradiation of the surface, and thermal radiation from the surface. Extrapolating YORP acceleration timescales estimated by Rubincam (2000), the expected value for 2006 HY51 is  $\sim 10^6$  yr. Analytical approximations of the YORP effect as a function of orbital parameters, mass, shape, and stellar luminosity (Scheeres 2007; Veras & Scheeres 2020), within the great uncertainty of many parameters, provide estimates of the order of  $0.1$ – $1.0 n$  per year, which should be enough to remove the asteroid out of a

high-spin resonance. Observationally, however, only much lower accelerations have been detected not exceeding  $7 \times 10^{-6}$   $\text{rad day}^{-1} \text{yr}^{-1}$  for the Cacus asteroid (Đurech et al. 2018). These estimates refer to objects in smaller orbits with lower eccentricity (up to 0.5). The YORP effect for extremely high eccentricity is an absolutely unexplored area of research. The solar irradiation is better approximated with impulse-like bursts at perihelia, and a monotonic acceleration model (spin-up or spin-down) is not obvious. Furthermore, once the asteroid is captured in a spin-orbit resonance, its orientation is not random at perihelia, where most of the energy deposition takes place. Depending on the specific free libration pattern, one side of the asteroid may be heated more than the other as long as the resonance lasts. This violates the starting assumption (which is probably valid for the chaotic stage) that the asteroid absorbs energy equally from all sides. The condition of anisotropic irradiation may have far-reaching consequences, which are difficult to guess without detailed modeling and simulation.

A state of resonance may be relatively short-lived for other reasons besides YORP acceleration. Gravitational interactions with major planets, even of limited magnitude, can change the orbital parameters (eccentricity and pericenter distance, most importantly) and violate the conditions of resonance. It is reasonable to assume that a sudden change of the eccentricity, for example, can make a specific resonance at the high end of spin rates unstable, and the object embarks on another extended chaotic journey. Even more likely, landslides, micrometeorite impacts, and other stochastic physical processes conspire to regulate the spin, up and down, throughout the evolution.

#### 4. Three Kinds of High-spin Resonances

Regular circulation resonances constitute approximately 2/3 of our trials and are characterized by the same apoastron and periastron  $\theta$  modulo  $\pi$ , which can be close to 0 or  $\pi$  (aligned) or  $\pi/2$  (sidewise), and a stable, weakly librating aphelion rotation velocity.<sup>9</sup> It is noted that in the aligned apoastron orientation, the geometrically longest axis of the asteroid is aligned with the direction to the primary attractor, while a sidewise orientation is reached when the shortest equatorial axis is aligned with that direction. The best known example of the latter in the solar system is Mercury, which is sidewise aligned at aphelia. The amplitude of free libration is limited by the width of a particular resonance. The remaining 1/3 of cases represent two new kinds of spin-orbit resonance, which may not have been described in the literature.

The first new kind, called switching resonance, is characterized by a nearly constant aphelion velocity  $\omega$ , which is in a higher order of commensurability  $f$  with the mean motion  $n$ , and aphelion orientation cycling through integer multiples of  $\pi/f$ . One example is the resonance at  $\omega = 1042.25n$  (i.e., 4169:4,  $f = 4$ ). The spin rate appears to chaotically vary within a very narrow range of  $0.0006n$  around the mean value, while  $\theta_{\text{aphelion}}$  modulo  $\pi$  switches between  $\pi/4$  and  $3\pi/4$  between each consecutive orbit; see Figure 6. The blue circles show the aphelion normalized orientation angles, while the red circles show the perihelion angles. The dashed lines do not represent the actual behavior of  $\theta$  between the apsides but serve only to help the eye to see the switching behavior. Obviously, this

<sup>9</sup> We call it *circulation* resonance to emphasize the continuously high prograde spin, which is only perturbed with high-amplitude pulses at perihelion passages. The closest well-known example of circulation resonance is Mercury, albeit with a much slower rotation at 3:2 commensurability.

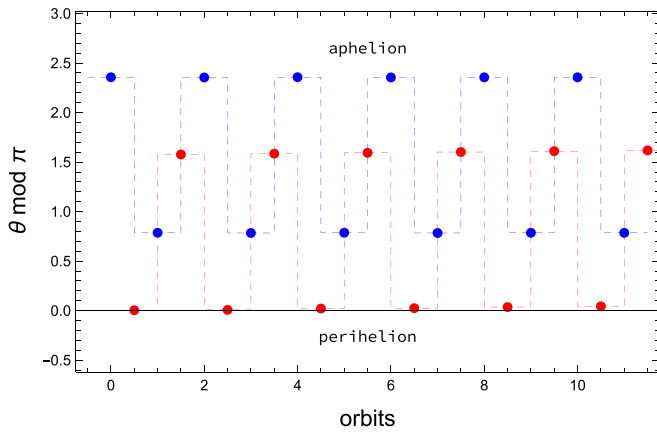


**Figure 6.** Aphelion (blue) and perihelion (red) orientation angles  $\theta$  modulo  $\pi$  in the 4169:4 *switching* spin-orbit resonance of 2006 HY51.

resonance is only possible when the numerator of the spin-orbit commensurability is an odd integer. The aphelion tilt of  $45^\circ$  with respect to the Sun’s direction compensates the fractional part of the relative spin, to the effect that the perihelion orientation angle switches between  $\pi/2$  (sidewise) and  $\pi$  (aligned) in increments of integer multiple of  $\pi/2$ . Our simulations indicate that this resonance is rarely achieved through chaotic evolution, probably due to its narrowness. Although this switching of orientation may be considered to be a high-order case of the general spin-orbit commensurability, no analogs exist in the low-eccentricity solar system, with Mercury having the highest order of commensurability 3:2 (Noyelles et al. 2014), but still not switching its orientation. High-order resonances ( $f > 2$ ) may be common in known tightly packed exoplanet systems where a planet’s eccentricity may be excited by gravitational interaction with other planets (e.g., Makarov et al. 2012). Surviving exoplanets orbiting white dwarfs may also be captured into this kind of resonance, but its condition in the  $\sigma$ - $e$  space remains to be investigated.

The second new kind, called jumping resonance, is characterized by a nearly constant aphelion orientation  $\theta$  modulo  $\pi$ , which is close to  $\pi/2$  (sidewise), and aphelion velocity jumping between two quantum states for each pair of orbits, separated from an exact commensurability by a finite value. The possibility of a stable spin-orbit resonance with noncommensurate spin rate has never been proposed, even theoretically. One example is the resonance at  $\omega = 958.57923n$  alternating with  $958.42041n$ , shown in Figure 7. As in the previous graph, the stepwise broken line is shown only to help the eye to visualize the alternating aphelion spin rate. The actual integrated curve is close to this broken line everywhere except the short time spans of a few days around perihelion passages, where the spin rate undergoes powerful variations much greater in amplitude than the range of this plot. The aphelion orientation angle (not presented for brevity) shows a random process-like variation within a very narrow range without any signs of a periodic libration-like modulation. From our massive simulations of chaotic trajectories with random initial conditions, this noncommensurate resonance appears to be rarer (i.e., has a lower probability of capture) than the regular circulation resonance possibly because of the narrow range in  $\theta$ . The offset of  $\omega$  from the commensurate fraction causes the asteroid to enter the perihelion at a slight tilt of its longest axis to the direction to the Sun. The tilt causes an asymmetric impulse driving  $\omega$  to the other quantum state,

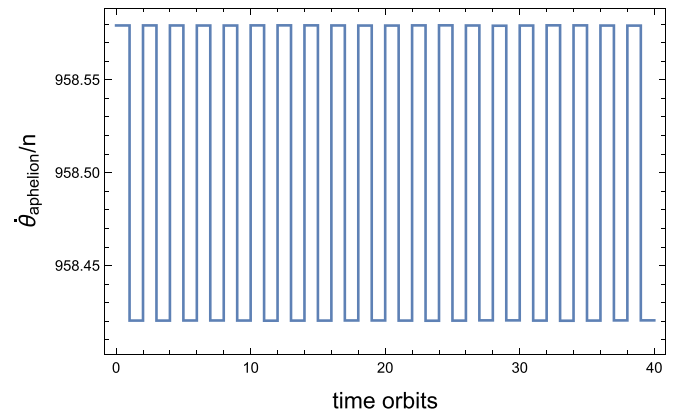


**Figure 7.** Aphelion rotation velocity in the  $(958.5 \pm 0.079)n$  *jumping* spin-orbit resonance of 2006 HY51 obtained from high-accuracy numerical integration of the ODE of motion.

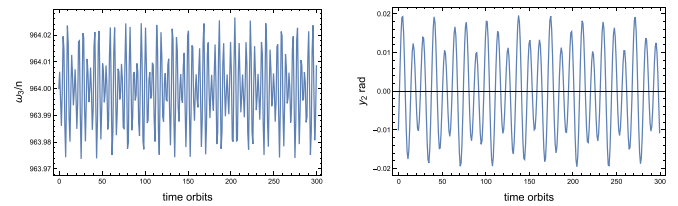


**Figure 8.** Aphelion rotation velocity (left) and pitch angle (right) in the 964: 1 spin-orbit resonance of 2006 HY51 obtained from high-accuracy numerical integration of the 3D Euler’s equations of motion.

resulting in a tilt with the opposite sign at the next perihelion passage. Amazingly, this jumping equilibrium is stable, in that a small perturbation in either parameter does not result in a larger change of aphelion parameters.

## 5. Inroads into the Full 3D Case

Full 3D simulations of Euler’s equations are in order to check the stability of high-spin resonances in the presence of obliquity wobble. The challenges are more daunting in 3D because of the immense parameter space that has to be mapped to locate and measure the resonances. Besides the six initial condition parameters (orientation angle and spin rate for each axis), the results are quite sensitive to eccentricity, orbital frequency, and relative distribution of the moments of inertia. The three Euler’s equations of rotation including Coriolis accelerations should be solved simultaneously as a single system of ODEs. This dramatically raises the computing cost of simulations. Our fast chaotic trajectory simulation method cannot be used, and other numerical methods have to be exploited to distinguish chaotic trajectories from deterministic states.

We performed limited 3D simulations to verify some of the resonances described in this paper. Figure 8 shows the results of a full-scale numerical integration for 2006 HY51 with stiffness switching for 300 orbits (1251 yr). The initial conditions for the starting point at aphelion are  $y_1 = -0.01$  rad,  $y_2 = -0.01$  rad,  $y_3 = \pi$  rad,  $\omega_1 = 0.01 n$ ,  $\omega_2 = -0.005 n$ ,  $\omega_3 = 964 n$ . The triaxial inertia coefficients are  $(B - A)/C = 0.1611$ ,  $(C - A)/B = 0.3423$ ,  $(C - B)/A = 0.1918$ . The left panel displays the evolution of normalized spin rate around the principal axis of the largest inertia moment at aphelia. The right panel shows the evolution of one of the orientation angles (pitch) also at aphelia. Both functions display a complex pattern of free libration with amplitudes of up

to  $0.024n$  and  $0.02$  rad, respectively. The important conclusion is that the 964:1 spin-orbit resonance is real and long-term stable in the absence of external perturbations. However, if we try to significantly increase the initial deviations of spin rates from these values, we obtain trajectories that show initially small perturbations, which exponentially grow in amplitude as the object literally begins to spin out of control in about 200 orbits. This implies that the investigated resonance is rather narrow in terms of initial orientation angles and spin. Consequently, the characteristic times of capture and chaotic evolution may become longer in 3D, and the life expectation inside the resonance may become shorter. It remains to be seen if other equilibria exist at  $\omega_3 = 964n$  and nonzero commensurate spin rates in the other two dimensions.

## 6. Conclusions

By simulating chaotic rotation of high-eccentricity asteroids with our fast-tuple-generating method for 1 Gyr time intervals, we discovered the existence of high spin-orbit resonances. These stable resonances may serve as protection against rotational breakup at higher eccentricity, which needs to be investigated separately. Apart from the regular circulation resonances maintaining nearly constant aphelion velocity and orientation angle, we discovered two new kinds of spin-orbit resonances: a switching resonance alternating the orientation angle, and a noncommensurate jumping resonance alternating the aphelion velocity between two quantum states. All three kinds are intrinsically stable, but the disposition of specific commensurabilities and the width of spin-orbit resonances are both eccentricity and triaxiality dependent, which is demonstrated for the regular 964:1 resonance using a chaos detection method.

The characteristic times of capture with 2006 HY51 parameters are well below 100 Myr. Therefore, 2006 HY51 may be captured in one of such resonances, which would be interesting to verify by observation. Rotation period can be inferred from systematic photometric observations, and two campaigns bracketing a perihelion conjunction could reveal whether the asteroid maintained a resonance velocity and its value. On the other hand, if 2006 HY51 happens to be in the chaotic state of rotation, a significant and measurable update

could be observed. Because of the narrowness of these equilibrium states, a moderate external perturbation (from an inner planet, for example) may extract the asteroid and trigger another chaotic walk for millions of years.

D.V. gratefully acknowledges the support of the STFC via an Ernest Rutherford Fellowship (grant ST/P003850/1). We used Julia (Rackauckas & Nie 2017) to implement our chaotic rotation simulation method, which is available as open-source software via GitHub.

## ORCID iDs

Valeri V. Makarov  <https://orcid.org/0000-0003-2336-7887>  
Dimitri Veras  <https://orcid.org/0000-0001-8014-6162>

## References

- Danby, J. M. A. 1962, *Fundamentals of Celestial Mechanics* (New York: MacMillan)
- Datseris, G. 2018, *JOSS*, **23**, 598
- Debes, J. H., Walsh, K. J., & Stark, C. 2012, *ApJ*, **747**, 148
- Đurech, J., Vokrouhlický, D., & Pravec, P. 2018, *A&A*, **609**, A86
- Goldreich, P., & Peale, S. 1966, *AJ*, **71**, 425
- Hestroffer, D., Sánchez, P., Staron, L., et al. 2019, *A&ARv*, **27**, 6
- Jura, M. 2003, *ApJL*, **584**, L91
- Koester, D., Gänsicke, B. T., & Farihi, J. 2014, *A&A*, **566**, A34
- Makarov, V. V., Berghea, C., & Efroimsky, M. 2012, *ApJ*, **761**, 83
- Makarov, V. V., Goldin, A., & Veras, D. 2020, *ApJ*, **899**, 103
- Makarov, V. V., & Veras, D. 2019, *ApJ*, **886**, 127
- Malamud, U., & Perets, H. B. 2020a, *MNRAS*, **492**, 5561
- Malamud, U., & Perets, H. B. 2020b, *MNRAS*, **493**, 698
- Noyelles, B., Frouard, J., Makarov, V. V., et al. 2014, *Icar*, **241**, 26
- Rackauckas, C., & Nie, Q. 2017, *JORS*, **5**, 15
- Rubincam, D. P. 2000, *Icar*, **148**, 2
- Scheeres, D. J. 2007, *Icar*, **188**, 430
- Skokos, Ch., Bountis, T. C., & Antonopoulos, Ch. 2007, *PhyD*, **231**, 30
- Veras, D., Leinhardt, Z. M., Bonsor, A., & Gänsicke, B. T. 2014, *MNRAS*, **445**, 2244
- Veras, D., McDonald, C. H., & Makarov, V. V. 2020, *MNRAS*, **492**, 5291
- Veras, D., & Scheeres, D. J. 2020, *MNRAS*, **492**, 2437
- Wisdom, J. 1987, *AJ*, **94**, 1350
- Wisdom, J., Peale, S. J., & Mignard, F. 1984, *Icar*, **58**, 137
- Zuckerman, B., Melis, C., Klein, B., Koester, D., & Jura, M. 2010, *ApJ*, **722**, 725